

## THE EVOLUTION OF LOW-REDSHIFT GALAXY STRUCTURES

MONIKA BIERNACKA<sup>1</sup>, PIOTR FLIN<sup>1</sup>, AND ELENA PANKO<sup>2</sup>

<sup>1</sup> Jan Kochanowski University, Kielce, Poland; [bmonika@ujk.kielce.pl](mailto:bmonika@ujk.kielce.pl), [sfflin@cyf-kr.edu.pl](mailto:sfflin@cyf-kr.edu.pl)

<sup>2</sup> Department of Astronomy, Odessa National University, Ukraine; [tajgeta@sp.mk.ua](mailto:tajgeta@sp.mk.ua)

Received 2008 December 10; accepted 2009 February 21; published 2009 April 27

### ABSTRACT

Ellipticities for 6188 low-redshift ( $z < 0.18$ ) poor and rich galaxy structures have been examined along with their evolution using an optical observational base that is statistically complete. The shape of each structure projected on the celestial sphere was determined using the covariance ellipse method. Analysis of the data indicates that structure ellipticity changes with redshift, being smaller for nearby objects and greater for those located further away. Such a change is also described better by quadratic or exponential relations than by a simple linear scheme. It is concluded that between redshifts of  $z = 0.18$  and  $z = 0$  we observe the dynamical evolution of galaxy clusters. Such a change in ellipticity with redshift is expected in  $\Lambda$ CDM models.

*Key words:* galaxies: clusters: general – galaxies: evolution – large-scale structure of universe

### 1. INTRODUCTION

The shape of galaxy clusters has been investigated by several authors, with several papers published since 1980 in which cluster ellipticity was determined using both optical and X-ray data. In all papers an elongated shape of the structures was reported; see the historical summary presented by Sereno et al. (2006). An ellipse was used as an approximation for the shape of the galaxy cluster structures observed in projection on the celestial sphere, the determination of apparent structure ellipticity being the main goal of such studies. More recently, investigators have attempted to establish the intrinsic, three-dimensional shapes of such structures from the distribution of apparent ellipticities in the structures.

Melott et al. (2001) analyzed a sample of galaxy clusters, using data from both X-ray and optical studies. The resulting sample contained about 160 rich galaxy clusters, in which the signature of a redshift–ellipticity relation was found, the ellipticity increasing with redshift. Melott et al. (2001) interpreted the effect as confirmation of the hierarchical clustering scenario in a low- $\Omega_m$  universe. In such a universe, the accretion of matter along protostructure filaments causes newly created structures to be very elongated. The subsequent merging and infall of matter later cause such clusters to be more nearly spherical. The similar processes are expected in the  $\Lambda$ CDM (Hopkins et al. 2005).

Plionis (2002) used a much larger sample in his study. In the optical region (see Figure 2 of Plionis) there are more than 400 APM clusters (Dalton et al. 1997), for which Plionis found a correlation between cluster ellipticity and redshift for  $z \leq 0.15$ . His interpretation of the result was similar to that of Melott et al. (2001), namely, that recent gravitational relaxation causes cluster sphericity.

Cluster eccentricity and temporal evolution were studied in two further papers by Floor et al. (2003, 2004). They compared the evolution of galaxy clusters in different numerical simulations with the observed data set, but did not find temporal evolution in their simulations ( $z < 0.13$ ). Instead, they found very slow evolution in simulated galaxy clusters, much weaker than what is observed. That could be the result of either observational bias or incomplete physics in the simulations. The analysis was criticized because it compared results for various regions of both observed and simulated clusters (Rahman et al.

2006). Lack of evidence for an ellipticity–redshift correlation was reported by Flin et al. (2004) when a collection of 246 ACO clusters (Abell et al. 1989) was analyzed, but Rahman et al. (2006) pointed out that in fact a weak correlation is observed when the change  $de/dz$  is considered for various radii of the investigated clusters. An application of the Faint Object Classification and Analysis System package (Jarvis & Tyson 1981) to the Digitized Sky Survey produced a new sample of 377 ACO clusters with  $z < 0.2$  and  $|b| > 40^\circ$ . From different methods Biernacka (2007) found a strong signature for the temporal evolution of galaxy cluster ellipticity.

Hopkins et al. (2005) performed numerical simulations in  $\Lambda$ CDM cosmology that are useful to such an analysis. They examined the evolution of ellipticity for galaxy clusters as a function of redshift, performing  $N$ -body high-resolution simulations for three-dimensional clusters, repeating them for the case of projection “in order to allow direct comparison with future observations.”

The aim of the present paper is to compare theoretical predictions with observational data arising from a new, statistically complete catalog of low-redshift galaxy clusters. The paper is organized in the standard fashion. Section 2 presents the observational data, Section 3 categorizes the change of ellipticity with redshift, and conclusions are presented at the end.

### 2. OBSERVATIONAL DATA

#### 2.1. The Catalog of Galaxy Structures

The PF Catalog of galaxy structures (hereafter PFCat; Panko & Flin 2006) is the observational basis for the present study. The catalog was created using data from the Muenster Red Sky Survey (hereafter MRSS; Ungruhe et al. 2003), which is a large-scale galaxy catalog covering an area of about 5000 deg<sup>2</sup> in the southern hemisphere, complete to a magnitude limit of  $r_F = 18.3$  mag. The same magnitude limit defines the completeness limit for galaxies in the PFCat. The MRSS is the result of scanning 217 ESO plates with  $b < -45^\circ$ .

The two-dimensional Voronoi tessellation technique (Ramella et al. 1999, 2001; Panko & Flin 2006) was applied to the galaxy catalog to search for overdense regions. The resulting PFCat includes 6188 such structures, with at least 10 galaxies in each structure field. The Voronoi procedure gives only the area and equivalent radius for the overdense structures, while the PF-

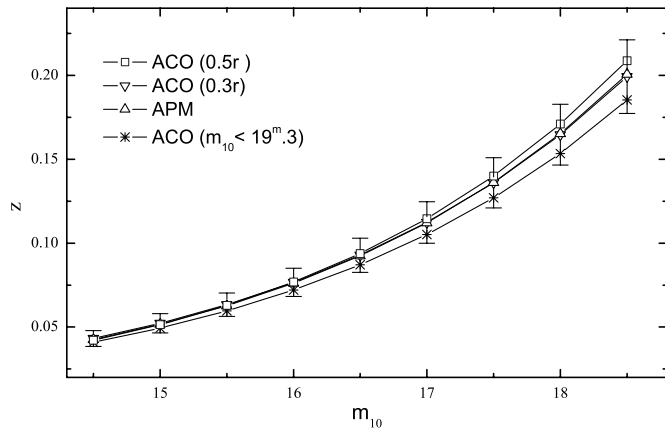


**Figure 1.** Variations of the estimated redshift  $z$  for values of the coefficients in Table 1. All other values lie inside the uncertainties of the selected dependence 2 (ACO 0.3r).

Cat contains information about their shape and orientation on the celestial sphere. A covariance ellipse method involving five moments for the distribution of galaxy coordinates was used to calculate the elliptical shape describing each structure as well as the position angle of its long axis. Lists of galaxies in the magnitude range  $m_3$  to  $m_3 + 3$  mag, where  $m_3$  is the brightness of the third brightest galaxy in the structure area, and the rectangular coordinates  $x$  and  $y$  of the galaxies were employed for the calculation of the semiaxes  $a$  and  $b$  of the resulting ellipses, the ellipticity parameter  $e = 1 - \frac{b}{a}$ , and the position angle of each structure’s long axis.

2.2. Distance Calibration

Since the MRSS does not contain galaxy distances, in order to obtain distance estimates for the PF structures, we calibrated the  $(\log z) - m_{10}$  relation following Dalton et al. (1997). The first step of the procedure was to compare the positions of the structure centers, as given in the PFCat, with those in the ACO and APM cluster catalogs. If the distance between the centers of the PF and ACO clusters was less than 0.5 of the PF equivalent cluster radius, the two objects were regarded as identical. More than 1000 such identifications were found. Only 466 ACO clusters from the list have measured redshifts  $z$  in NED. The calibration of the  $(\log z) - m_{10}$  relation in the form

$$\log z_{\text{est}} = a + b \cdot m_{10} \tag{1}$$

is based on 455 data points. Excluded from the analysis were 11 data points, mainly clusters with small redshifts, because of apparent misfit, probably caused by erroneous structure identification. The structure identification was repeated using a value of 0.3 of the PF cluster radius as a new criterion of identity. That produced a similar relationship, but based on a smaller number of center coincidences.

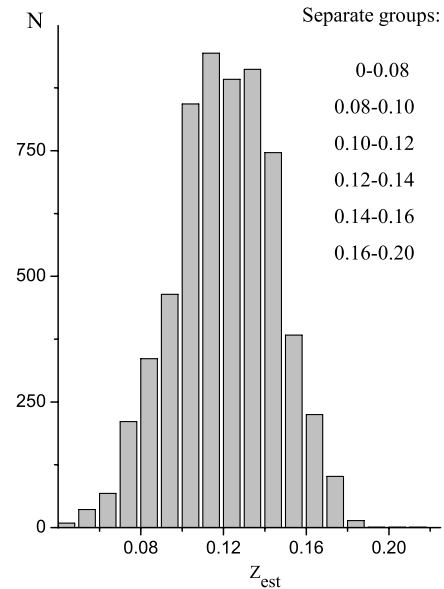


**Figure 2.** Distribution of estimated  $z$  and the limits of the division into groups.

We repeated the procedure with data for APM clusters, taking the measured redshift  $z$  from the APM cluster catalog (Dalton et al. 1997). Additional calibration of the  $\log z_{\text{est}} - m_{10}$  relation was possible through comparison of a deeper version of the PFCat with the ACO catalog. The deeper version of the catalog is not statistically complete because the limiting magnitude of galaxies considered is  $r_F = 19.3$  mag. Table 1 summarizes the best fits obtained from four estimated redshift calibrations. Column 2 of the table lists four variants of the structure identification described above. Columns 3 and 4 list resulting values for the coefficients  $a$  and  $b$  of calibration relation (Equation (1)) together with their uncertainties (in brackets) on the lower line. Columns 5, 6, and 7 contain the number of identified clusters, the standard deviation (s.d.) for the relationship, and the correlation coefficient  $R$  in each case. For future work we select the relation

$$\log z_{\text{est}} = -3.771 + 0.1660 \cdot m_{10}, \tag{2}$$

corresponding to the relationship given in line 2 of Table 1.

All of the various investigated relationships are plotted in Figure 1. Note that each particular relation is located within the confidence limits for the other relations. Dependences 2 and 3 show best agreement over the full magnitude interval, but even the most discordant relations, as in cases 1 and 4, give a maximal difference in  $z_{\text{est}}$  of only 0.02 for a magnitude limit of  $m = 18.3$  mag.

3. THE CHANGE OF STRUCTURE ELLIPTICITY WITH REDSHIFT

For structures in the PFCat, the estimated values of redshift  $z$  are less than 0.20. A histogram showing the distribution of

**Table 1**  
The Result of the Statistical Analysis for the  $m_{10} - z$  Relationship

$N$	Identification for Input Data	$a$	$b$	Number	s.d.	$R$
1	ACO (0.5r)	-3.895(±0.210)	0.1737(±0.012)	455	0.17	0.56
2	ACO (0.3r)	-3.771(±0.242)	0.1660(±0.015)	290	0.17	0.55
3	APM (0.5r)	-3.813(±0.148)	0.1684(±0.009)	372	0.11	0.65
4	ACO ( $m_{10} < 19^m.3$ )	-3.767(±0.195)	0.1641(±0.0116)	519	0.18	0.28

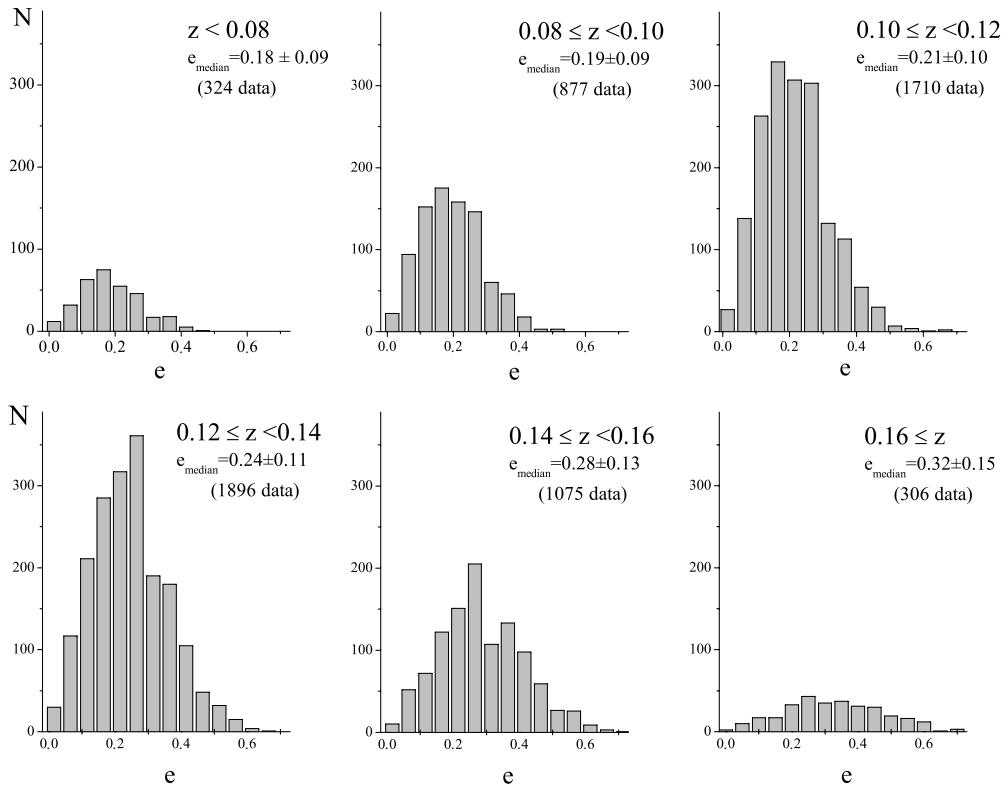


Figure 3. Distribution of ellipticity in different redshift groups.

structures in the PFCat according to a given redshift  $z_{\text{est}}$  is presented in Figure 2. The  $e-z$  relation was investigated for all 6188 structures in the catalog, and the parameters were found to be correlated at the  $\alpha = 0.95$  significance level. For further study of the ellipticity variations, the sample of 6188 structures was divided into six groups with different redshifts. The two extreme groups were amalgamated because of small sample size, with the width of the redshift interval being  $\Delta z = 0.02$  for the remaining groups. The median ellipticity and s.d. for each redshift group are presented in Figure 3.

The median value of ellipticity for PF structures is  $0.23 \pm 0.12$  (Panko & Flin 2006), a value that can be attributed to the large number of PF structures with estimated redshifts between 0.10 and 0.15. The distributions of ellipticity within each separate group are shown in Figure 3.

The increase of mean ellipticity with redshift is clearly seen in the calculated values of the median ellipticity as well as in the distributions presented in Figure 3. The dependence of median group ellipticity on redshift is summarized in Figure 4. Both linear and nonlinear fits were applied to the  $e-z$  relation, and for the nonlinear fit, both quadratic and exponential relations were employed. The results displayed good agreement with the data for both types of nonlinear fits.

The correlation coefficients for linear, quadratic, and exponential fits are 0.975, 0.998, and 0.997, with s.d.s of  $\pm 0.014$ ,  $\pm 0.003$ , and  $\pm 0.004$ , respectively. The differences between the two investigated nonlinear fits are so small that it is difficult to state which is better, although both are clearly superior to a simple linear fit. It appears reasonable to conclude that the ellipticity–redshift relationship is nonlinear in character. The frequency of highly elongated structures quickly increases when  $z > 0.14$ .

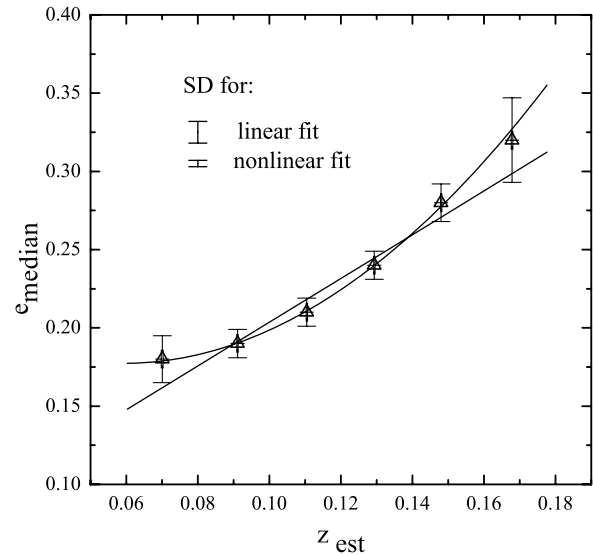


Figure 4. Change of the median value of structure ellipticity with redshift.

#### 4. CONCLUSIONS

A catalog of low-redshift galaxy cluster structures has been constructed that is statistically complete to about  $z < 0.18$ . A particular advantage of the original galaxy catalog is the fact that automatic star/galaxy image separation was afterward checked visually, which significantly lowered the number of incorrectly classified objects. The structure finding was performed through application of the Voronoi tessellation technique, which is regarded as the optimum method for finding both spherically symmetric and nonsymmetric structures. The results of its application are commonly accepted (Kim et al. 2002). The

shape of the galaxy cluster structures was determined using the classical covariance ellipse method.

In Biernacka (2007), Monte Carlo simulations using 500 clusters for each ellipticity ( $e = 0.0, 0.1, \dots, 0.9$ ) were employed in modeling galaxy clusters. Two shape finders were applied to each generated structure, namely, using the covariance ellipse and the Minkowski functional methods. Both techniques systematically underestimated the calculated ellipticity in comparison with the actual value for the generated clusters. The variance of the calculated ellipticities was smaller for the covariance ellipse method than for the case of the second method employed. It therefore appears that the covariance ellipse method is a good tool for cluster ellipticity studies.

In a similar fashion the shapes of poor and rich galaxy cluster structures were calculated, which ensures a similar approach to both. The ellipticity change with redshift was analyzed here, with the result that the median structure ellipticity is found to increase with redshift. The observed relation is nonlinear in character, and the number of elongated structures grows rapidly when  $z > 0.14$ . It can be surmised that, in the case of nearby galaxy cluster structures, the effect of dynamical evolution is observed. Nearer structures are more nearly round, which can be attributed to virialization processes occurring in the not so distant past. From the shape of the redshift–ellipticity dependence one can speculate that in the past ( $0.14 < z < 0.18$ ) such processes were more intense than at present. As shown by numerical simulations in  $\Lambda$ CDM cosmology, such a change of ellipticity with redshift is expected. Although a detailed analysis of the problem was performed by Hopkins et al. (2005), the present results cannot be compared directly with the theoretical predictions. Numerical simulations dealt with massive clusters out to redshift  $z = 3$ , while the present analysis was confined to low-redshift galaxy cluster structures that included both poor groups and

very rich clusters. Nevertheless, the present results indicate that structure elongation increases with redshift, which is in agreement with the general trend reported in the numerical simulations.

The present research has made use of the NASA/IPAC Extragalactic Database (NED), which is operated by the Jet Propulsion Laboratory, California Institute of Technology, under contract with the National Aeronautics and Space. This research has also made use of NASA's Astrophysics Data System. The present research was partially supported by the Jan Kochanowski University grants BS 052/08 and BW116/08.

## REFERENCES

- Abell, G. O., Corwin, H. G., & Olowin, R. P. 1989, *ApJS*, **70**, 1  
 Biernacka, M. 2007, PhD thesis, Univ. Lodz  
 Dalton, G. B., Maddox, S. J., Sutherland, W. J., & Efsthathiou, G. 1997, *MNRAS*, **289**, 263  
 Flin, P., Krywult, J., & Biernacka, M. 2004, in Proc. IAU Coll. 195, *Outskirts of Galaxy Clusters: Intense Live in the Suburbs*, ed. A. Diaferio (Cambridge: Cambridge Univ. Press), 248  
 Floor, S. N., Melott, A. L., Miller, C. J., & Bryan, G. L. 2003, *ApJ*, **591**, 741  
 Floor, S. N., Melott, A. L., & Motl, P. M. 2004, *ApJ*, **611**, 153  
 Hopkins, P. F., Bahcall, N. A., & Bode, P. 2005, *ApJ*, **618**, 1  
 Jarvis, J. F., & Tyson, J. A. 1981, *AJ*, **86**, 476  
 Kim, R. S. J., et al. 2002, *AJ*, **123**, 20  
 Melott, A. L., Chambers, S. W., & Miller, C. J. 2001, *ApJ*, **559**, L75  
 Panko, E., & Flin, P. 2006, *J. Astron. Data*, **12**, 1  
 Plionis, M. 2002, *ApJ*, **572**, L67  
 Rahman, N., Krywult, J., Motl, P. M., Flin, P., & Shandarin, S. F. 2006, *MNRAS*, **367**, 838  
 Ramella, M., Boschin, W., Fadda, D., & Nonino, M. 2001, *A&A*, **368**, 776  
 Ramella, M., Nonino, M., Boschin, W., & Fadda, D. 1999, in ASP Conf. Ser. 176, *Observational Cosmology: The Development of Galaxy Systems*, ed. G. Giuricin, M. Mezzetti, & P. Salucci (San Francisco, CA: ASP), 108  
 Sereno, M., De Filippis, E., Longo, G., & Bautz, M. W. 2006, *ApJ*, **645**, 170  
 Ungruhe, R., Seitter, W. C., & Duerbeck, H. W. 2003, *J. Astron. Data*, **9**, 1